

# Selective adsorption of azine group containing pesticides on carbon-based materials

Pooja,<sup>1</sup> Pamthingla Ragui,<sup>1</sup> Pratibha Kumari,<sup>\*2</sup> Rakesh K. Sharma<sup>\*1</sup>

<sup>1</sup>Department of Chemistry, University of Delhi, New Delhi, India. <sup>2</sup>Department of Chemistry, Deshbandhu College, University of Delhi, New Delhi, India.

Submitted on: 05-Nov-2024, Accepted and Published on: 01-Jan-2025

Article

## ABSTRACT

Adsorption of atrazine (ATR) and diquat (DIQ) pesticides were studied on two carbon-based adsorbent materials, graphene oxide (GO) and activated carbon (AC). A modified synthesis of graphene oxide has also been developed using phosphoric acid in reduced amounts instead of nitric acid to reduce the formation of poisonous by-products such as nitrogen oxides which are harmful environmental contaminants. High selectivity in DIQ and ATR removal studies was observed with GO and AC. The GO showed more adsorption efficiency for DIQ (97.99 %) whereas AC was more selective for ATR removal (99.99 %). The selectivity of pesticides was accredited to the interplay of surface area and surface charge. The Langmuir adsorption isotherm was followed by all the adsorption studies and the BET isotherm was also obeyed in the case of selective adsorption of DIQ by GO and ATR by AC. The pseudo-second-order kinetics was observed in all adsorption studies and the value of the amount adsorbed at equilibrium ( $q_e$ ) was found to be similar theoretically and experimentally.



**Keywords:** Graphene oxide, activated charcoal, atrazine, diquat, adsorption, water treatment, remediation, pesticides

## INTRODUCTION

The mounting problem of water pollution has been a major concern as clean water is the basic necessity for the survival of life on earth. A World Economic Forum report in 2019 indicated that around 70% of water in India is not fit for human consumption<sup>1</sup> and clean water is one of the crucial Sustainable Development Goals (SDG) of the United Nations Development Programme (UNDP). However, in the last five decades, there have been about twenty-six times increments in the usage of pesticides in the agriculture field to fulfill the needs of growing populations<sup>2</sup>. Therefore, their persistence in the environment poses a serious threat to human health. Among various water purification methods, adsorption is one of the simplest, most efficient, and economical methods for

water purification. Various materials have been developed, especially, activated carbons, graphene oxide, chitosan, and zeolite for the removal of various pollutants from water through adsorption. The potential of carbon-based material for the selective removal of various contaminants needs to be explored more for the development of task-specific water treatment strategies.

Atrazine (ATR) and Diquat (DIQ) are the two most commonly used azine group containing herbicides. They are found largely in water bodies in more than their permissible limits, threatening aquatic lives due to their excessive use and negligence in regulation. The acute toxicity of ATR is caused by the metabolism of ATR which prevents fish antioxidant enzyme activities resulting in oxidative stress and promoting mitochondrial damage-causing carp neutrophilic granulocyte apoptosis.<sup>3</sup> DIQ is highly water-soluble and its toxicity is mainly caused by its tendency to propagate reactive oxygen species. There have been several reported cases of DIQ poisoning in humans worldwide which is mostly of intentional ingestion. Therefore, the removal of these pesticides from water is very important. Diquat is removed from aqueous solutions by adsorption onto activated carbon fabric,<sup>4</sup> magnetic and non-magnetic carbon nanotube-based adsorbents, and

<sup>\*</sup>Corresponding Author: Pratibha Kumari, Rakesh K. Sharma  
Email: pratibhatanwar77@gmail.com (PK), sharmark101@yahoo.com (RKS)

Cite as: J. Integr. Sci. Technol., 2025, 13(3), 1061.  
URN:NBN:sciencein.jist.2025.v13.1061  
DOI:10.62110/sciencein.jist.2025.v13.1061



©Authors CC4-NC-ND, ScienceIN <https://pubs.thesciencein.org/jist>

oxidized multiwalled carbon nanotube (OMWCNT) have been reported<sup>5</sup>. Removal of endocrine-disrupting pesticide, atrazine by adsorption was done on various adsorbents such as modified zeolite<sup>6</sup>, and magnetic covalent organic framework. However, there is a growing demand to develop a system for the efficient and selective removal of these pesticides.

Carbon-based adsorbents are gaining more popularity as they are economical, easily available, and possess high adsorption efficiency. AC is the most widely used carbonaceous material for removing various contaminants from water.<sup>7</sup> The process by which pollutants adhere to the surface of AC through  $\pi$ - $\pi$  interactions, hydrogen bonding, van der Waals interaction, and cation/ anion- $\pi$  interactions is primarily responsible for their water remediation action.<sup>8</sup> GO is another widely used carbon material that is getting commercial importance for water treatment applications, however, there is a sweltering need to explore its potential for selective water contaminants removal so that the area-specific water pollution problem can be solved.

The selective adsorption using GO or modified GO of dyes,<sup>9</sup> lysozyme, and heavy metals such as cadmium, uranium, chromium, and lead<sup>10</sup> are widely studied however there are not much-reported studies on the selective adsorption of pesticides. There are limited studies that involved the use of GO and modified GO for the removal of pesticides such as endrin and dieldrin,<sup>11</sup> dichlorodiphenyldichloroethylene,<sup>12</sup> and chlorinated pesticides<sup>13</sup> however, the dosage and contact time in these studies are relatively more. Activated carbon with various modifications is a very well-known and extensively used adsorbent for the removal of various contaminants from wastewater.<sup>14</sup> Few reports depict the removal of pesticides such as organophosphorus, chlorinated pesticides<sup>15</sup>, triazine pesticides, and chlorophenoxy pesticides using activated charcoal, however, no selectivity was observed in the removal of pesticides. There is still a burgeoning demand for extensive removal studies of pesticides from water samples using economical and easily available materials to provide commercial-level water treatment solutions to mankind.

Herein, we report the modified synthesis of GO using phosphoric acid and the application of AC and GO in the removal of two widely used pesticides, ATR and DIQ. The adsorption behavior of the pesticides on the adsorbents was studied as a function of the amount of adsorbent and time by batch experiments using a UV-visible spectrophotometer. Adsorption data were fitted to Freundlich, Langmuir, and BET isotherms to study adsorption. Pseudo-first and second-order kinetic models were also fitted.

## EXPERIMENTAL

All commercial-grade chemicals and solvents were purchased and used as received. Double distilled water was used in all preparations and the adsorption studies. HCl, H<sub>2</sub>SO<sub>4</sub>, hydrogen peroxide, and, KMnO<sub>4</sub> were purchased from Rankem. *ortho*-H<sub>3</sub>PO<sub>4</sub>(HPLC grade) from Spectrochem, activated charcoal (AC) from Qualigen, and graphite powder was purchased from CDH. The Infrared Spectroscopy (IR) data were recorded on the Shimadzu IR Affinity instrument. The Raman Spectroscopy analysis was carried out on the Renishaw Laser Raman Spectrometer and the UV- Visible Spectroscopy studies were

performed on the Shimadzu UV-61 UV Visible spectrophotometer. The BET Surface area analyzer was used to record the surface area of materials using the Quantachrome Instruments ASI-CI-11 instrument. The Field Emission Scanning Electron Microscope (FESEM) data were recorded on Zeiss Gemini SEM 500. The Scanning Electron Microscopy analysis was done on JEOL Japan Mode: JSM 6610LV. The Transmission Electron Microscopy was performed on the Thermo Scientific Technai G20 HRTEM instrument. The Tabletop XRD Olympus BTX-561 model was used for the X-ray Diffractometer data.

### Synthesis of graphene oxide

The enhanced Hummer process was modified to create graphene oxide.<sup>16</sup> Graphite powder(1g) was added to a stirring mixture of concentrated sulphuric acid (25mL) and orthophosphoric acid (2.77mL), in a ratio of 9:1 in a round bottom flask. It was stirred well at room temperature. After proper mixing, the reaction mixture was transferred to an ice bath. Once the reaction mixture was cooled, KMnO<sub>4</sub>(3g) was added very slowly. The reaction was further continued in an ice bath for 30 minutes and later allowed to stir at room temperature for 3 hours. Then, 50 mL of water was added dropwise with the help of a dropping funnel to maintain a constant flow of water drop by drop and also for safety reasons as the addition of water to acid is a highly exothermic reaction. 100 ml water was again added to the reaction mixture and then 5 mL 30% H<sub>2</sub>O<sub>2</sub> was added to stop the oxidation reaction by reacting with the excess potassium permanganate. A bright yellow colour developed in the reaction mixture. The reaction mixture was kept undisturbed overnight at room temperature and the product was separated by centrifugation at 8100 rpm for 10 minutes followed by washing with 5% HCl three to four times and then with water. The separated graphene oxide was dried at 70 °C for 48 hr.

### Adsorption experiments

Aqueous stock solutions of ATR and DIQ (10ppm) were prepared in double-distilled water. Different dilutions of ATR and DIQ solutions with different concentrations (0.002–0.04 mmol L<sup>-1</sup>) were prepared by diluting the stock solution with water. The molar absorption coefficient ( $\epsilon$ ) was determined from the slope of absorbance (at 222nm for ATR and 310 nm for DIQ) vs concentration curve (standard curve) at room temperature.

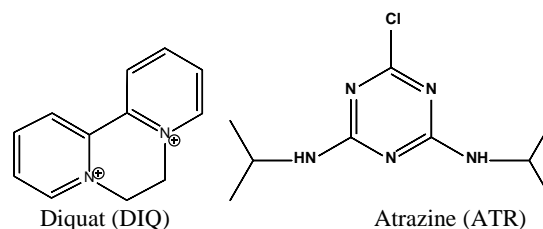


**Figure 1:** Structure of Diquat (DIQ) and Atrazine (ATR)

To a 25 mL solution of ATR or DIQ, adsorbent (GO or AC) was added in a varied amount (2.5mg - 10mg). The pesticide solutions and adsorbents were stirred on a magnetic stirrer continuously for a specified period and then the suspension was subjected to centrifugation at 10000 rpm for 8 minutes to measure the residual pesticides in the supernatant solution by recording its absorption spectra. The absorbance values were used to study kinetic models

(pseudo-first-order, pseudo-second-order) and adsorption models (intraparticle diffusion models, Freundlich adsorption, Langmuir adsorption, and BET adsorption model). The kinetic studies of adsorption were performed for up to 60 min in each set. The amounts of ATR or DIQ adsorbed on GO and AC were measured from the difference between the initial ( $C_0$ ) and equilibrium ( $C_e$ ) concentrations in the supernatant after centrifugation according to the equation:

$$q_e = (C_0 - C_e) \frac{V}{M}$$

Where  $q_e$ (mmolg<sup>-1</sup>) is the equilibrium adsorption capacity and  $V$  is the volume of pesticide solutions(L).  $M$  is the weight of the adsorbent used (g).

## RESULTS AND DISCUSSION

### Synthesis and Characterization of GO

Graphene oxide was synthesized by a slight modification of the Improved Hummer method (Figure S1). The present modified method affords GO at room temperature in less time. Graphite powder was treated with  $KMnO_4$  in a mixture of sulfuric acid and phosphoric acid (9:1). The synthesized graphene oxide was characterized by different techniques.

The powder X-ray diffraction pattern (Figure 2a) of synthesized GO showed a sharp peak at  $2\theta = 11.27^\circ$  due to the (002) plane of the GO structure<sup>17</sup>. The interlayer spacing ( $d$ ) was estimated to be 0.78 nm by well-established Bragg's law:

$$n\lambda = 2d\sin\theta$$

where  $n$  is the diffraction series and  $\lambda$  is the diffraction wavelength.

According to reports, the interlayer spacing value for graphene oxide (GO) ranges from 0.6 to 1.0, indicating the extent of oxidation and the number of water molecules incorporated into the interlayer spacing.<sup>18</sup> Therefore, the value of 0.78 nm of interlayer spacing can be attributed to the highly oxidized form of graphite, indicating the formation of GO from graphite. The FTIR spectrum of GO (Figure 2b) confirmed the presence of functional groups and the formation of GO from graphite. A broad band around  $3400\text{cm}^{-1}$  is attributed to O-H stretching which is involved in hydrogen bonding and a band at  $1710\text{cm}^{-1}$  confirms the presence of a carboxylic acid functional group in GO. The band between  $1000\text{cm}^{-1}$  to  $1250\text{cm}^{-1}$  corresponds to C-O-C epoxy bonds and the vibrational mode of C-O groups.<sup>19</sup> The band between  $1300\text{-}1400\text{cm}^{-1}$  is characteristic of C=C aromatic bonds. The Raman spectrum (Figure 2c) showed two distinct bands: D band ( $1370\text{cm}^{-1}$ ) and G band ( $1598\text{cm}^{-1}$ ) which is in line with the literature values for GO.<sup>20</sup> The D band arises due to disordered structure and the intensity of the D band is smaller because of the breakage of stacking order of graphite after oxidation whereas the G band arises due to stretching of the C-C bond in graphitic materials.<sup>19</sup> The UV visible spectrum of GO (Figure 2d) also showed characteristic absorption bands. A well-built absorption peak at  $233\text{nm}$  corresponding to  $\pi\text{-}\pi^*$  transition of aromatic C=C structure and a weak shoulder peak at  $305\text{nm}$  corresponding to  $n\text{-}\pi^*$  transition of carbonyl bonds<sup>19</sup> confirms the GO formation in the reaction.

The morphology of GO was studied by the SEM, FESEM, and TEM analysis (Figure 3). The SEM and FESEM images were recorded at  $10\text{ }\mu\text{m}$ . The SEM image depicted the surface topography of GO i.e., the stacking of several layers of GO (Figure

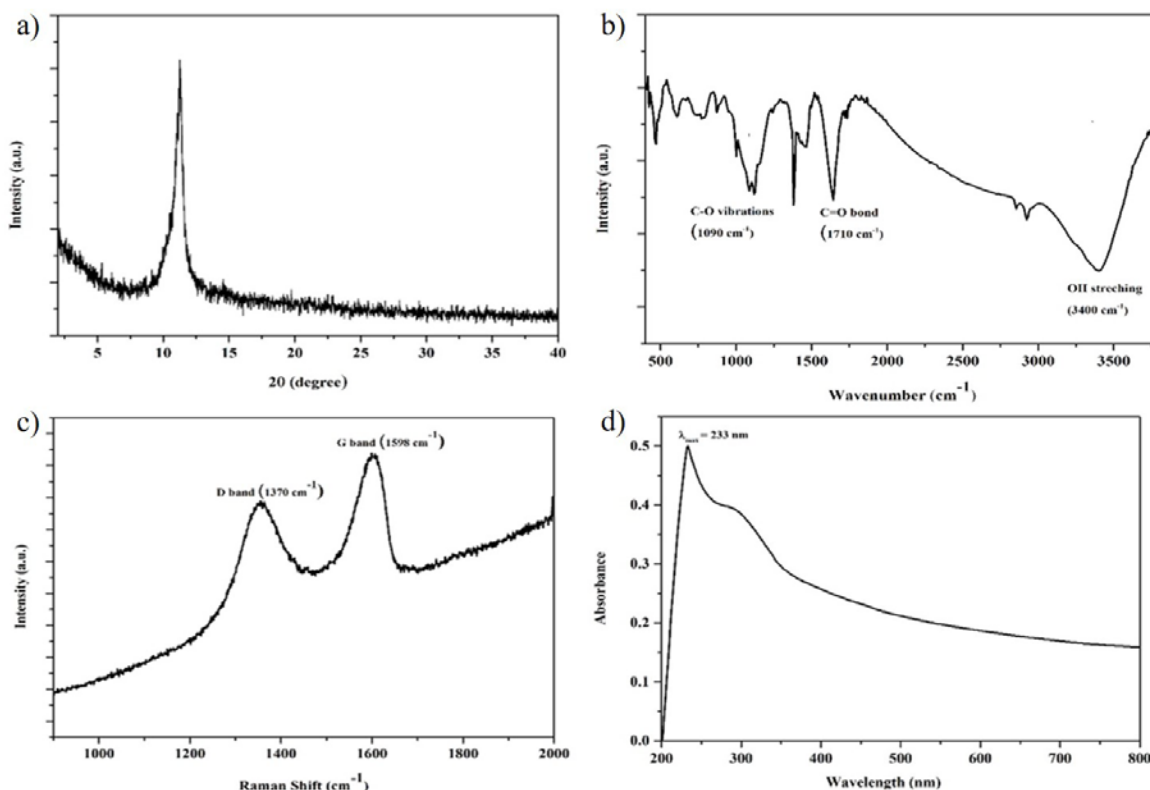


**Figure 2:** Characterization data for GO a) XRD pattern b) IR spectrum c) Raman spectrum d) UV-Vis spectra.

3a). The FESEM images showed a pile of GO sheets (Figure 3b). The layers of GO sheets are seen at lower magnification. The EDAX data stipulated towards non-appearance of other impurities in the material (Figure 3c). The TEM image (Figure 3d) was recorded at a magnification of  $1\mu\text{m}$  at which the distinctive ripples

of GO sheets are visible which validates the graphenic nature of the synthesized material.<sup>21</sup>

### Absorption studies using GO and AC

#### Effect of different dosages of adsorbents

Different dosage studies of adsorbents were carried out to optimize the conditions.

Three variable amounts of adsorbent (10 mg, 5 mg, and 2.5 mg) were used in adsorption studies (Figure S3, S4) and the adsorption efficiency (%) has been summarised in Table S1. The optimum amount of adsorbent that showed the highest adsorption efficiency is 10 mg for both GO and AC under experimental conditions. To understand the adsorption mechanism, all the other studies such as UV, IR, XRD, etc are performed with 10 mg of adsorbent.

#### Time-dependent adsorption studies

The adsorption studies were performed for two carbon-based adsorbents, activated charcoal (AC) and graphene oxide (GO) under different conditions for two model pesticides, diquat and atrazine. The elimination of ATR and DIQ pesticides from aqueous solutions utilizing GO and AC was studied using a UV-visible spectrophotometer. The absorbance peaks at 222nm and 310nm in the UV range are for ATR and DIQ<sup>22</sup> respectively, which were used to monitor the removal of pesticides (Figure 4). In all sets of experiments, the adsorption was studied for 60 minutes each. 10 mg of GO extracted 97.49% of DIQ and 74.91 % ATR in 60 minutes from an aqueous solution whereas the same amount of AC on the other hand, extracted 99.99% of ATR and 25.88 % DIQ in 60

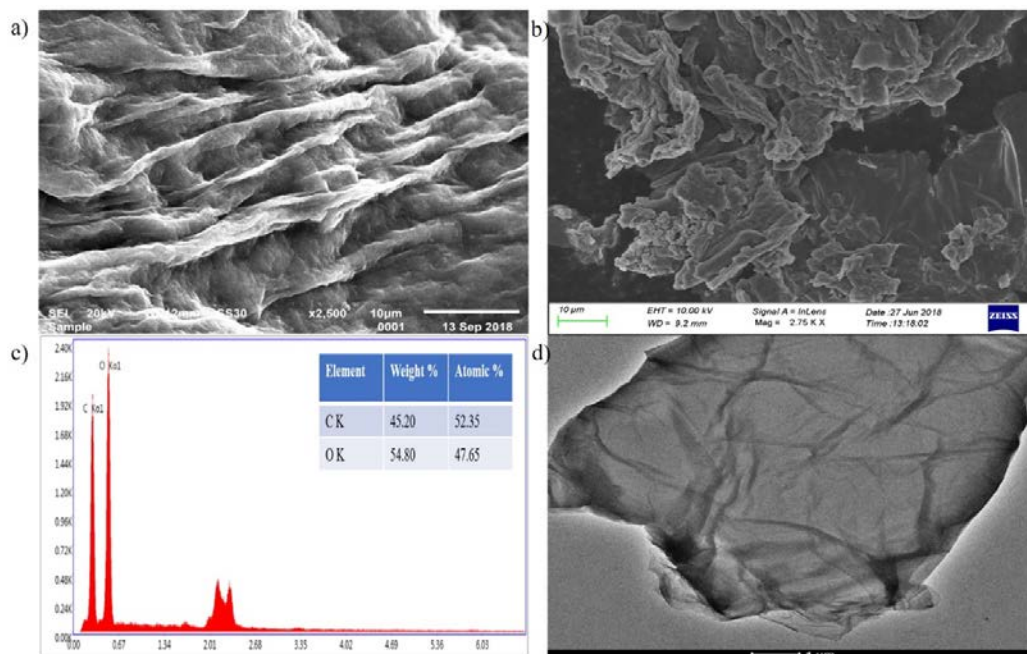


**Figure 3:** Characterization of GO a) SEM image b) FESEM image c) EDAX spectra d) TEM image of GO

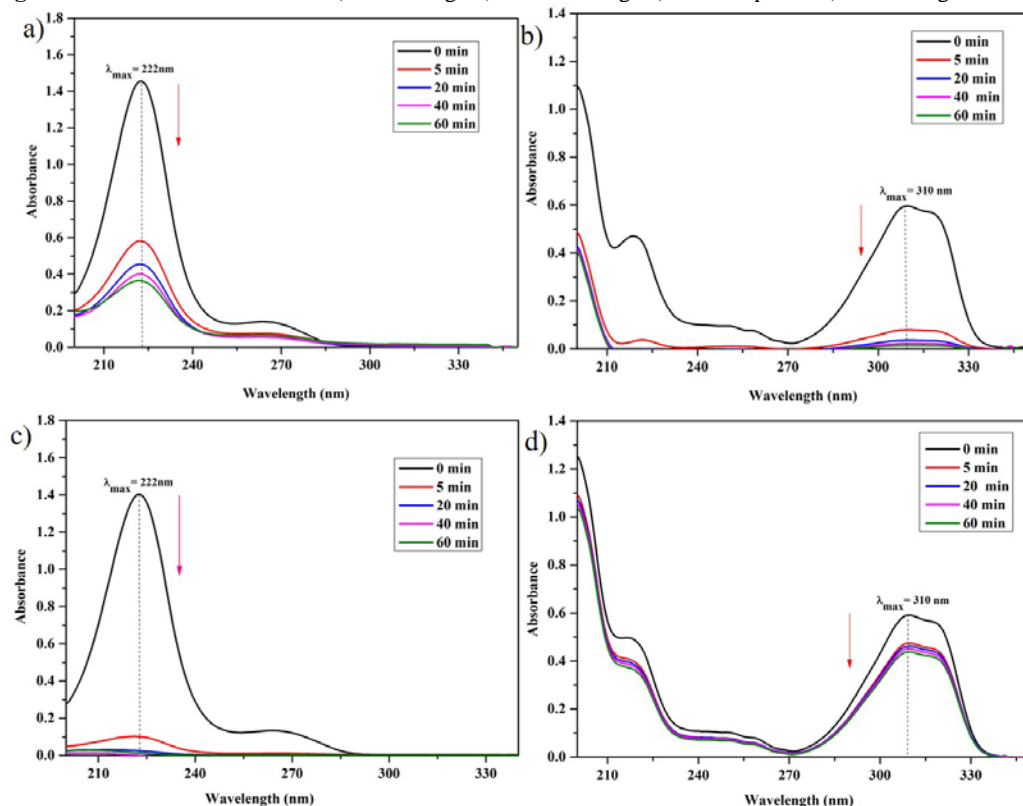


**Figure 4:** Time dependent UV-Visible spectra of [a] ATR(25 ml of 10ppm solution) with GO(10 mg).[b] DIQ (25 ml of 10ppm solution) with GO(10 mg).[c]ATR(25 ml of 10ppm solution) with AC(10 mg).[d] DIQ(25 ml of 10ppm solution) with AC (10 mg)

minutes. GO appeared to be selective for DIQ while AC appeared to be selective for ATR.

GO being a nanomaterial has a high surface area in comparison to AC due to which it adsorbed ATR with 53.30% efficiency even though it had a similar surface charge. AC depicted only 25.88% removal efficiency for DIQ, this can be attributed to a similar surface charge and low surface area as compared to GO.<sup>23</sup>

GO adsorbs almost all of DIQ in the initial 5 minutes whereas it does not adsorb ATR completely even after 60 minutes. GO carries a negative surface charge<sup>24</sup> and DIQ is a positively charged<sup>25</sup> herbicide, therefore, the electrostatic force of attraction worked synergistically with other interactive forces such as H-bonding and facilitated the adsorption process. ATR, on the other hand, bears a negative surface charge<sup>23</sup>, therefore, on exposing it to an aqueous solution of GO the adsorption process takes place but the rate of adsorption is slow because of a similar surface charge. GO is a well-known adsorbent as it possesses high surface area and porosity. The above results show that surface charge and surface area both have a cooperative effect on the rate and amount of adsorption.

AC also being a carbon-based adsorbent is well known for adsorption. It has a positive charge on its surface.<sup>26</sup> Among the adsorbates, AC adsorbed almost a complete amount of ATR within the first 5 minutes of the experiment whereas it could not even adsorb 30% of DIQ in 60 minutes of the experiment. The rate of adsorption of adsorbents GO and AC irrespective of surface charge can be compared based on the surface area. GO being a nanomaterial has a comparatively higher surface area than AC which has its size range in  $\mu\text{m}$  scale. If we consider only the surface area as the basis of adsorption, GO is a far better adsorbent than AC but when surface charge comes into play then the rate and amount of adsorption is an interplay of both surface area and surface charge. The electrostatic force of interaction has a very high effect on the process of adsorption and due to this, GO and AC are established to be highly selective adsorbents towards DIQ and ATR, respectively. If we consider only the surface charge as the basis and ignore surface area then GO adsorbs ATR in 60 minutes because of a similar surface charge. AC has comparatively less surface area than GO and also a similar charge as DIQ it could not adsorb even a small amount of DIQ in 60 minutes.

#### Adsorption Mechanism

To understand the adsorption of model

contaminants by GO, we performed spectroscopic studies of adsorbents after the completion of the adsorption process under present conditions. Figure 5a shows a TEM image of adsorbent GO at a scale of 200nm before adsorption of pesticide which shows plain rippled layers of GO sheets. The surface of the adsorbent has free sites and pores for adsorption. Figure 5b indicates that the surface of the adsorbent is not free but is covered with DIQ and the particles of DIQ are evident on the surface after adsorption on GO sheets. The shape of the sheet seems to be altered a sign of aggregation appeared. -COOH and -OH groups exist in GO which leads to a negative surface charge on the surface of GO.<sup>27</sup> Adsorption of ionic species leads to alterations on the surface. As the pesticide under study here DIQ has a positive surface charge (Figure S2) so its adsorption leads to the neutralization of charge and aggregation. On the contrary, if adsorption of neutral species is carried out it does not lead to any surface charge and therefore no aggregation.<sup>21</sup>

The XRD comparison of adsorbent GO with and without adsorbate was also studied (Figure 5c). Diffractograms of GO showed its characteristic peak at 11.27. The XRD spectra recorded after the adsorption of both pesticides indicated all the shreds of evidence of adsorption such as a decrease in intensity, shifting of a peak, and appearance of some new peaks which affirmed the adsorption of pesticides over adsorbent.<sup>28</sup> The process of adsorption also affects the crystallinity of GO as the peak corresponding to the (002) plane decreases in intensity and is displaced towards a lower angle also some new humps appeared at higher angles which hinted toward interstratifications. The former can be attributed to disorientations across the axis or rearrangement of atoms from their positions.<sup>29</sup> The latter can be accredited to the

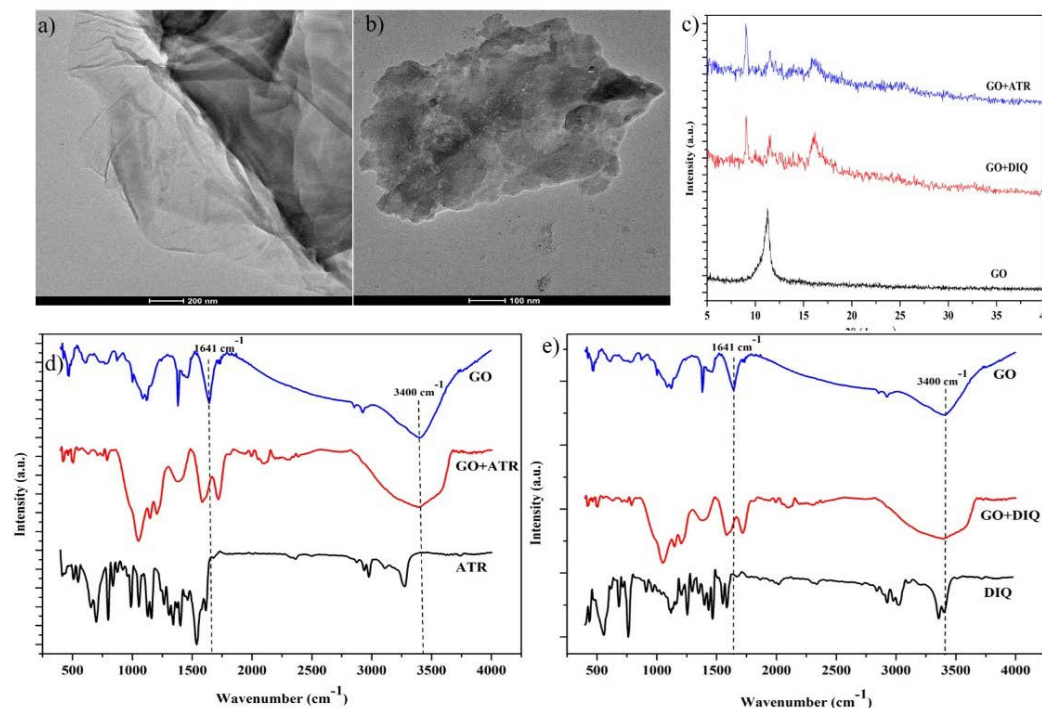


**Figure 5:** Comparison of GO with and without DIQ and ATR a) TEM image without pesticide b) TEM image of GO+ DIQ c) Comparative IR of GO, GO+ ATR and ATR d) Comparative IR of GO, GO+DIQ, DIQ

shrinkage of some layers which in turn is due to the expansion of other layers.<sup>30</sup> The peak hinting towards interstratifications is less intense and broad suggesting complex interstratifications.<sup>31</sup>

Infrared spectra of ATR, DIQ, GO, and GO after adsorption of ATR and DIQ were studied (Figure 5d,5e). IR spectra of ATR showed its characteristic peaks as reported in the literature.<sup>32</sup> Some major peaks of the triazine group are around 1540 cm<sup>-1</sup> and N-H stretching around 3250 cm<sup>-1</sup>. The IR spectra of DIQ also followed the literature values.<sup>33</sup> The broadening of O-H stretching in IR spectra of GO after adsorption of pesticide established the statement that pesticides were adsorbed on GO by H-bonding between hydroxyl and carboxyl group of GO sheets and nitrogen functionality of pesticides. The broadening of O-H stretching is more in the case of DIQ as compared to ATR which also supports adsorption isotherm and time-dependent studies that GO selectively adsorbs DIQ better than ATR through H-bonding.<sup>34</sup> The established peak of the carbonyl group around 1640 cm<sup>-1</sup> in GO also gets affected by the interaction of pesticide with GO as it also assists the process of adsorption by π-π interactions involving the carbonyl group.<sup>35</sup> Therefore, IR spectral studies confirmed that the adsorption of pesticides was a synergistic effect of H-bonding and π-π interactions.<sup>36</sup>

**Adsorption Isotherms**

The adsorption experiments were studied by Freundlich(ln q<sub>e</sub> vs ln C<sub>e</sub>)(Figure S4 ), Langmuir (C<sub>e</sub>/q<sub>e</sub> vs C<sub>e</sub>) (Figure 6) and BET (C<sub>e</sub>/C<sub>0</sub> vs C<sub>e</sub>/C<sub>0</sub>) (Figure S5 ) adsorption isotherms. Adsorption isotherms were studied for 60 min. The linear equations for Freundlich, Langmuir, and BET isotherms are stated in Eqn. 1,2 and 3 respectively.<sup>37</sup> C<sub>e</sub>(mmol L<sup>-1</sup>) is the equilibrium concentration of pesticides, q<sub>max</sub> (mmolg<sup>-1</sup>) in Langmuir isotherm stands for maximum adsorption capacity, q<sub>e</sub> (mmolg<sup>-1</sup>) is the amount adsorbed at equilibrium, k<sub>F</sub>(mmol<sup>1-n</sup>L<sup>n</sup>g<sup>-1</sup>),k<sub>L</sub>(Lmmol<sup>-1</sup>) stand for Freundlich and Langmuir constants respectively. B, C in Eqn. 3 are constants, x<sub>m</sub> is the amount of pesticide required to form the monolayer over the surface of the adsorbent, and n stands for adsorption intensity.<sup>38</sup>

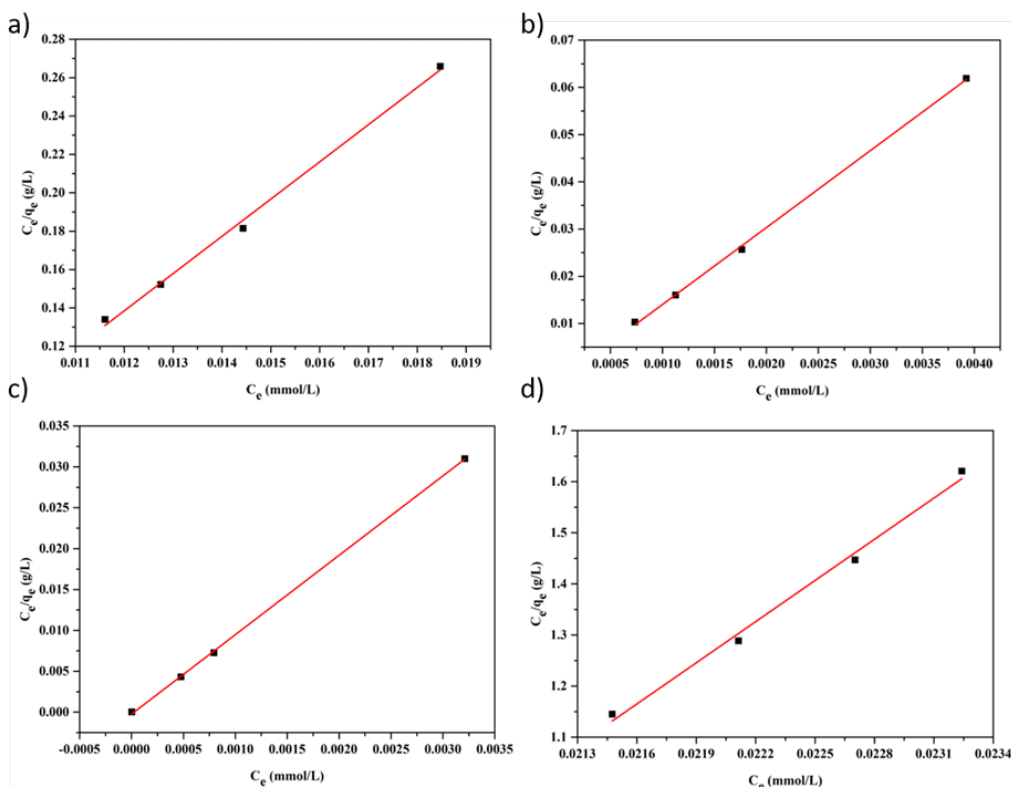


**Figure 6:** Langmuir Adsorption isotherm for a) ATR on GO b) DIQ on GO c) ATR on AC d) DIQ on AC

**Table 1:** Freundlich, Langmuir and BET isotherm of Adsorbents (AC and GO) for pesticides (ATR and DIQ) adsorption

		Freundlich isotherm			Langmuir isotherm				BET isotherm		
Adsorbent (10 mg)	Pesticides	k <sub>F</sub> (mmol <sup>1-n</sup> L <sup>n</sup> g <sup>-1</sup> )	n	R <sup>2</sup>	k <sub>L</sub> (Lmmol <sup>-1</sup> )	q <sub>max</sub> (mmol g <sup>-1</sup> )	R <sup>2</sup>	R <sub>L</sub>	x <sub>m</sub>	C	R <sup>2</sup>
AC	ATR	2.2851	0.0080	0.883	42215.2	0.103	0.9997	0.0005	0.095	948.35	0.999
	DIQ	16.989	3.3893	0.996	57.94	0.004	0.9905	0.09	0.0004	1.4835	0.977
GO	ATR	4.5795	0.4806	0.987	205.59	0.051	0.9952	0.37	0.0228	1.1537	0.932
	DIQ	3.1483	0.0719	0.916	7145.4	0.061	0.9990	0.004	0.051	113.96	0.996

Freundlich isotherm equation  $lnq_e = lnk_F + nlnC_e$  -----(1)

Slope: n Intercept:  $lnk_F$

Langmuir isotherm equation  $\frac{C_e}{q_e} = \frac{1}{k_L q_{max}} + \frac{C_e}{q_{max}}$  -----(2)

Slope:  $1/q_{max}$

Intercept:  $1/k_L q_{max}$

BET isotherm equation  $\frac{\frac{C_e}{C_0}}{q_e(1-\frac{C_e}{C_0})} = \frac{1}{x_m BC} + \frac{C-1}{x_m C}(C_e/C_0)$  -----(3)

Slope:  $\frac{C-1}{x_m C}$

Intercept:  $\frac{1}{x_m C}$

The comparison of regression coefficients among Freundlich and Langmuir in Table 1 suggests that the Langmuir isotherm is the best fit for all the adsorption experiments. Langmuir isotherm is based on assumption that the surface is homogeneous therefore, the very fact that Langmuir isotherm fits the data well consummate that there is a homogeneous distribution of active sites on the surface of the adsorbent. Freundlich isotherm depicts adsorption on the

inhomogeneous and rough surfaces<sup>39</sup> also adsorbent forms a monolayer on adsorbate surface.<sup>40</sup>

The R<sup>2</sup> for DIQ on AC and ATR on GO in Freundlich isotherm is 0.99 and 0.98 respectively i.e. these two sets of adsorptions closely relate to the Freundlich model. GO is functionalized with carboxylic acid and alcohol-based functional groups which attribute a negative surface charge and AC has more of a positive surface charge due to which they present homogeneous surface towards oppositely charged pesticides and consequently DIQ on GO and ATR on AC follow Langmuir isotherm well. The other two sets of adsorption's ATR on GO and DIQ on AC have a similar surface charge due to which they experience slight electrostatic repulsion and in turn inhomogeneous surface which explains the fact that they follow Freundlich adsorption isotherm.

The value of constants can be used to predict if adsorption is favorable or unfavorable. If the value of n (Eqn. 1) lies between 0 and 1 the process of adsorption is favorable and if n=0 then the process is irreversible and for n>1 the adsorption is highly unfavorable.<sup>41</sup> Table 2 shows that for AC+DIQ the value of n is 3.38 also for this % adsorption is 25% only, therefore, DIQ on AC is unfavorable adsorption. For all the other sets of experiments, n lies between 0 and 1.

Similarly for Langmuir isotherm, a separation factor R<sub>L</sub> can be defined

$$\text{where } R_L = \frac{1}{1 + k_L C_0}$$

The relation between R<sub>L</sub> and the favourability of adsorption can be described as if R<sub>L</sub> = 0 irreversible if 0<R<sub>L</sub><1 the adsorption is termed as favourable, and if R<sub>L</sub>>1 then adsorption is highly unfavourable.<sup>42</sup> Table 4 summarises the value of R<sub>L</sub> for adsorption studied. R<sub>L</sub> value for all the experiments lies between 0 and 1 i.e., all

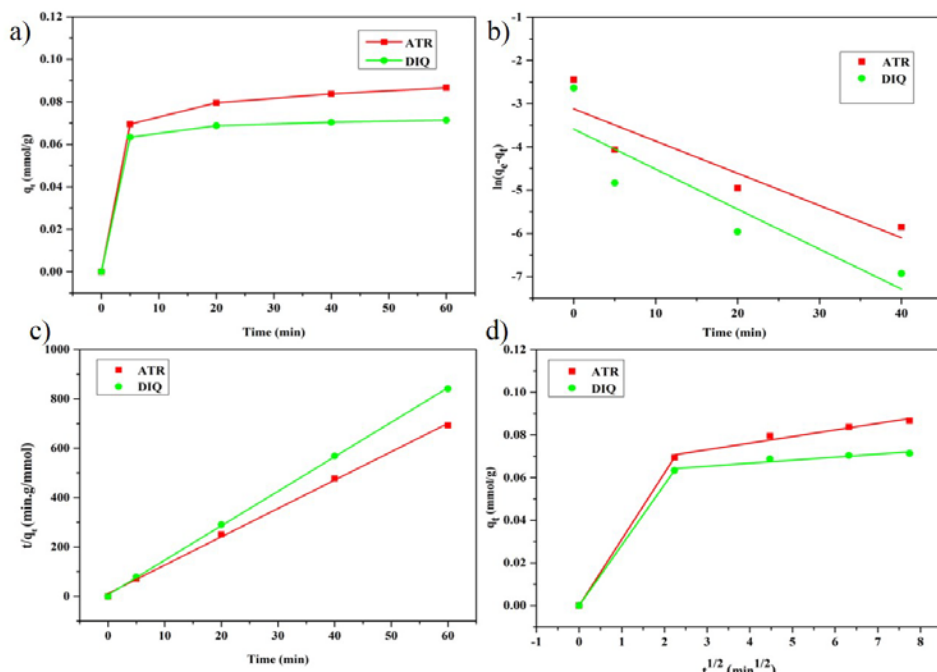


**Figure 7:** Adsorption kinetics for GO based on a) Amount adsorbed vs time b) Pseudo first order c) Pseudo second order d) Intraparticle diffusion model

the adsorption is favourable. For ATR on AC, the value is nearly 0 i.e., the adsorption is almost close to being irreversible.

The BET adsorption isotherm is an extension of the Langmuir isotherm and it assumes multilayer adsorption. The regression coefficients for DIQ on GO and ATR on AC portray that these studies follow both BET and Langmuir isotherms. This concluded that these adsorptions are multilayer followed by monolayer adsorption on the surface.<sup>37</sup>

**Adsorption Kinetic Models**

The adsorption kinetics were studied by three different models by plotting  $\ln(q_e - q_t)$  vs  $\ln q_e$  for pseudo first-order and  $\frac{t}{q_t}$  vs  $t$  for pseudo second order and  $q_t$  vs  $t^{1/2}$  for intraparticle diffusion model (IPDM). Equations corresponding to every model were fitted to the data and studied respectively.<sup>37</sup>

Pseudo first-order equation  $\ln(q_e - q_t) = \ln q_e - k_1 t$ -----  
-----(4)

Slope:  $-k_1$  Intercept:  $\ln q_e$

Pseudo second-order equation  $\frac{t}{q_t} = \frac{1}{k_2 q_e^2} + \frac{t}{q_e}$ -----  
-----(5)

**Table 2:** Kinetic parameters of pseudo-First order, pseudo second-order, and Weber-Morris Models for ATR and DIQ on Activated Charcoal (C<sub>0</sub>=10 ppm, Adsorbent (AC and GO), T= 25°C, pH ~7)

Adsorbent (0.01g)	Pesticides	Pseudo first order			Pseudo second order				Intraparticle diffusion model		
		k <sub>1</sub> (min <sup>-1</sup> )	q <sub>e</sub> (mmolg <sup>-1</sup> )	R <sup>2</sup>	k <sub>2</sub> (min <sup>-1</sup> )	q <sub>e</sub> (mmol g <sup>-1</sup> ) (expt.)	q <sub>e</sub> (mmol g <sup>-1</sup> ) (theor.)	R <sup>2</sup>	k <sub>i</sub> (mmolg <sup>-1</sup> min <sup>-0.5</sup> )	I (mmol g <sup>-1</sup> )	R <sup>2</sup>
AC	ATR	0.09647	0.03245	0.58773	33.533	0.1117	0.1115	0.9999	0.0014	0.1015	0.80001
	DIQ	0.05065	0.01021	0.64261	30.124	0.01871	0.01875	0.9923	0.00078	0.01239	0.9724
GO	ATR	0.0745	0.0442	0.7733	11.3430	0.0871	0.08708	0.9996	0.00309	0.06382	0.94055
	DIQ	0.0925	0.0277	0.7186	29.864	0.0716	0.07134	0.9986	0.00143	0.06105	0.87337

Slope:  $1/q_e$  Intercept:  $\frac{1}{k_2 q_e^2}$

Intraparticle diffusion model  $q_t = k_i t^{1/2} + I$ -----(6)  
Slope:  $k_i$  Intercept: I

where t is time,  $q_e$  and  $q_t$  are amount adsorbed at equilibrium and time t respectively.  $k_1$ ,  $k_2$  and  $k_i$  are rate constants for pseudo first-order, pseudo second-order, and intraparticle diffusion models respectively. The slope and intercept values from Eqn 1 and 2 were used to evaluate the amount adsorbed at equilibrium ( $q_e$ ) was calculated theoretically as well as by first and second-order kinetics.

The rate constant values evaluated by eqn. 4,5 and 6 are tabulated in **Table 2**. **Figure 7b, 6c** and **Figure S7b, S7c** depicts pseudo first-order plots and pseudo second-order plots for GO and AC with both the pesticides and it is vividly evident that the adsorption process follows pseudo second-order kinetics much better than the first-order kinetics. Regression coefficients ( $R^2$ ) for first-order kinetics are very minimal whereas for pseudo second-order kinetics the values are higher than 0.99 in every case depicting that the linear fit is appreciably following pseudo second-order kinetics in all the adsorption experiments. The theoretical value of the amount adsorbed at equilibrium ( $q_e$ ) was also in accordance with experimental by second-order kinetics.

The intraparticle diffusion model given by Webber and Morris was used to study particles diffusion after surface adsorption.<sup>43</sup> The multilinearity of this curve suggests that the adsorption process takes place in two steps. Surface adsorption i.e. boundary diffusion takes place in the first step and the succeeding linear plot can be attributed to intraparticle diffusion all through the adsorbent.<sup>44</sup> The second linear part of the curve was utilized to elucidate the intraparticle diffusion parameter  $k_i$  ( $\text{mmol g}^{-1} \text{min}^{-0.5}$ ). I is the intercept as per Eqn. 3, it is evident from **Table 2** that **Figure 7d** and **S7d** that the first linear plot does not pass through origin suggesting IPD is not the only rate-determining step.<sup>38</sup> The value of I infers the boundary layer thickness.<sup>45</sup> The  $R^2$  values for all the studies were less than 0.97 suggesting the adsorption data does not follow IPDM that well. Yongmei Hao et al. reported<sup>46</sup> that GO- $\text{Fe}_3\text{O}_4$  could remove 96.6% DIQ whereas the present study showed 97.49% removal efficiency. Reported<sup>47,48</sup> studies that show the adsorption of pesticides does not focus on the selectivity for a specific pesticide which makes the present study significant.

## CONCLUSION

Modified synthesis of GO has been reported to afford a high yield of GO under mild conditions. The adsorption studies were performed for DIQ and ATR using GO and AC adsorbents which showed an appreciable amount of selectivity. 10 mg GO was found to adsorb 97.49% DIQ in 60 minutes at neutral pH and at room temperature whereas AC adsorbed 99.99 % ATR under the same conditions. On the contrary, the adsorption of ATR on GO was 74.91 % DIQ by AC was found to be 25.88 % only. GO and AC was highly selective towards DIQ and ATR respectively. This selective behaviour can be attributed to the surface charge of adsorbents. The adsorption isotherms studies made it very clear that all the adsorption studied are monolayer in nature as they all follow Langmuir isotherm. The non-selective one i.e. ATR on GO and

DIQ on AC having similar surface charges provides in-homogeneous surfaces for adsorption which in turn follow the Freundlich isotherm. The highly selective adsorption of ATR on AC and DIQ on GO is found to be multilayer by the BET adsorption studies. The kinetic studies revealed all adsorption studies follow pseudo second-order kinetics and the theoretical and experimental values of  $q_e$  were in correlation with each other up to the third decimal place for second-order kinetics.

## ACKNOWLEDGMENTS

The authors are highly thankful to CSIR, the Government of India, and the Institute of Eminence (IoE) University of Delhi (PP) for providing financial assistance and USIC for providing instrumental support. PK is thankful to the University Grants Commission, India for the UGC-BSR Research Start-Up Grant [F.30-311/2016 (BSR)] for providing financial assistance.

## CONFLICT OF INTEREST STATEMENT

Authors do not have any conflict of interest for this work.

## REFERENCES AND NOTES

- Water pollution is killing millions of Indians. Here's how technology and reliable data can change that | World Economic Forum <https://www.weforum.org/agenda/2019/10/water-pollution-in-india-data-tech-solution/> (accessed Nov 2, 2020).
- Atrazine in Drinking-water Background document for development of WHO Guidelines for Drinking-water Quality; **2003**.
- S. Wang, Q. Zhang, S. Zheng, et al. Atrazine exposure triggers common carp neutrophil apoptosis via the CYP450s/ROS pathway. *Fish Shellfish Immunol* **2019**, 84, 551–557.
- T. Tongur, E. Ayranci. Adsorption and electrosorption of paraquat, diquat and difenzoquat from aqueous solutions onto activated carbon cloth as monitored by in-situ uv-visible spectroscopy. *J Environ Chem Eng* **2021**, 9 (4), 105566.
- O. Duman, C. Özcan, T. Gürkan Polat, S. Tunç. Carbon nanotube-based magnetic and non-magnetic adsorbents for the high-efficiency removal of diquat dibromide herbicide from water: OMWCNT, OMWCNT- $\text{Fe}_3\text{O}_4$  and OMWCNT- $\kappa$ -carrageenan- $\text{Fe}_3\text{O}_4$  nanocomposites. *Environmental Pollution* **2019**, 244, 723–732.
- J. Lemić, D. Kovačević, M. Tomašević-Čanović, et al. Removal of atrazine, lindane and diazinone from water by organo-zeolites. *Water Res* **2006**, 40 (5), 1079–1085.
- R. Riaz, M. Ali, T. Maiyalagan, et al. Activated charcoal and reduced graphene sheets composite structure for highly electro-catalytically active counter electrode material and water treatment. *Int J Hydrogen Energy* **2020**, 45 (13), 7751–7763.
- M.J. Sweetman, S. May, N. Mebberson, et al. Activated Carbon, Carbon Nanotubes and Graphene: Materials and Composites for Advanced Water Purification. **2017**.
- S. Goyal, P. Ragui, A. Yadav, et al. A facile synthesis of bimetallic Ni/Co-BTC hollow MOFs for effective removal of congo red. *Sep Sci Technol* **2024**, 59 (10–14), 1202–1215.
- X. Li, Z. Wang, Q. Li, et al. Preparation, characterization, and application of mesoporous silica-grafted graphene oxide for highly selective lead adsorption. *Elsevier*.
- K. Shrivastava, A. Ghosale, N. Nirmalkar, et al. Removal of endrin and dieldrin isomeric pesticides through stereoselective adsorption behavior on the graphene oxide-magnetic nanoparticles. *Environmental Science and Pollution Research* **2017**, 24 (32), 24980–24988.
- A. M. Ismael, A. N. El-Shazly, S. E. Gaber, et al. Novel  $\text{TiO}_2/\text{GO}/\text{CuFe}_2\text{O}_4$  nanocomposite: a magnetic, reusable and visible-light-driven photocatalyst for efficient photocatalytic removal of chlorinated pesticides from wastewater. *RSC Adv* **2020**, 10 (57), 34806–34814.

13. K. Chatterjee, Alka, S. Kumar, R.K. Sharma, P. Kumari. Effective Removal of Nitrogenous Pesticides from Water Using Functionalized Calix[4]arene-Decorated Magnetite Nanoparticles. *Chemistry Select* **2023**, 8 (3), e202203426.
14. S. Budhiraja, A. Yadav, R.K. Sharma, \* Rakesh, K. Sharma. In-vitro cytotoxic studies of 1-hexylcarbamoyl-5-fluorouracil encapsulated nanogels in BMG-1 cells. *Chemical Biology Letters* **2024**, 11 (1), 655–655.
15. V.K. Gupta, B. Gupta, A. Rastogi, S. Agarwal, A. Nayak. Pesticides removal from waste water by activated carbon prepared from waste rubber tire. *Water Res* **2011**, 45 (13), 4047–4055.
16. D.C. Marcano, D. V. Kosynkin, J.M. Berlin, et al. Improved synthesis of graphene oxide. *ACS Nano* **2010**, 4 (8), 4806–4814.
17. N.M.S. Hidayah, W.W. Liu, C.W. Lai, et al. Comparison on graphite, graphene oxide and reduced graphene oxide: Synthesis and characterization. In *AIP Conference Proceedings*; American Institute of Physics Inc., **2017**; Vol. 1892.
18. D.C. Marcano, D. V. Kosynkin, J.M. Berlin, et al. Improved synthesis of graphene oxide. *ACS Nano* **2010**, 4 (8), 4806–4814.
19. D. Khalili. Graphene oxide: A promising carbocatalyst for the regioselective thiocyanation of aromatic amines, phenols, anisols and enolizable ketones by hydrogen peroxide/KSCN in water. *New Journal of Chemistry* **2016**, 40 (3), 2547–2553.
20. E.I. Bîru, H. Iovu. Graphene Nanocomposites Studied by Raman Spectroscopy. *Raman Spectroscopy* **2018**.
21. S.M. Maliyekkal, T.S. Sreepasad, D. Krishnan, et al. Graphene: A reusable substrate for unprecedented adsorption of pesticides. *Small* **2013**, 9 (2), 273–283.
22. R. Rial-Otero, B. Cancho-Grande, C. Perez-Lamela, J. Simal-Gándara, M. Arias-Estévez. Simultaneous determination of the herbicides diquat and paraquat in water. *J Chromatogr Sci* **2006**, 44 (9), 539–542.
23. L.C. Mahlalela, C. Casado, J. Marugán, et al. Photocatalytic degradation of atrazine in aqueous solution using hyperbranched polyethyleneimine templated morphologies of BiVO<sub>4</sub> fused with Bi<sub>2</sub>O<sub>3</sub>. *J Environ Chem Eng* **2020**, 8 (5), 104215.
24. M.J. Li, C.M. Liu, H. Bin Cao, Y. Zhang. Surface charge research of graphene oxide, chemically reduced graphene oxide and thermally exfoliated graphene oxide. In *Advanced Materials Research*; Trans Tech Publications Ltd, **2013**; Vol. 716, pp 127–131.
25. M. Pateiro-Moure, A. Bermúdez-Couso, D. Fernández-Calviño, et al. Paraquat and diquat sorption on iron oxide coated quartz particles and the effect of phosphates. *J Chem Eng Data* **2010**, 55 (8), 2668–2672.
26. J. Díaz-Terán, D.M. Nevskaja, A.J. López-Peinado, A. Jerez. Porosity and adsorption properties of an activated charcoal. *Colloids Surf A Physicochem Eng Asp* **2001**, 187–188, 167–175.
27. D. Li, M.B. Müller, S. Gilje, R.B. Kaner, G.G. Wallace. Processable aqueous dispersions of graphene nanosheets. *Nat Nanotechnol* **2008**, 3 (2), 101–105.
28. P.R. Rout, P. Bhunia, R.R. Dash. A mechanistic approach to evaluate the effectiveness of red soil as a natural adsorbent for phosphate removal from wastewater. *Desalination Water Treat* **2015**, 54 (2), 358–373.
29. E.D. Grayfer, A.S. Nazarov, V.G. Makotchenko, S.J. Kim, V.E. Fedorov. Chemically modified graphene sheets by functionalization of highly exfoliated graphite. *J Mater Chem* **2011**, 21 (10), 3410–3414.
30. D.M.C. MacEwan, A. Ruiz-Amil. Interstratified Clay Minerals. In *Soil Components*; Springer Berlin Heidelberg, **1975**; pp 265–334.
31. F. Barroso-Bujans, S. Cerveny, R. Verdejo, et al. Permanent adsorption of organic solvents in graphite oxide and its effect on the thermal exfoliation. *Carbon N Y* **2010**, 48 (4), 1079–1087.
32. Y. Kim, V.V. Shinde, D. Jeong, Y. Choi, S. Jung. Solubility enhancement of atrazine by complexation with cyclophosphorase isolated from *Rhizobium leguminosarum biovar trifolii* TA-1. *Polymers (Basel)* **2019**, 11 (3).
33. A.H. Kamel, A.E.G.E. Amr, N.S. Abdalla, et al. Modified screen-printed potentiometric sensors based on man-tailored biomimetics for diquat herbicide determination. *Int J Environ Res Public Health* **2020**, 17 (4).
34. T. Yamashita, K. Takatsuka. Hydrogen-bond assisted enormous broadening of infrared spectra of phenol-water cationic cluster: An ab initio mixed quantum-classical study. *Journal of Chemical Physics* **2007**, 126 (7), 74304.
35. P. Song, Z. Xu, Y. Wu, et al. Super-tough artificial nacre based on graphene oxide via synergistic interface interactions of  $\pi$ - $\pi$  stacking and hydrogen bonding. *Carbon N Y* **2017**, 111, 807–812.
36. B. Shen, W. Zhai, C. Chen, et al. Melt blending in situ enhances the interaction between polystyrene and graphene through  $\pi$ - $\pi$  Stacking. *ACS Appl Mater Interfaces* **2011**, 3 (8), 3103–3109.
37. X. Zhu, B. Li, J. Yang, et al. Effective adsorption and enhanced removal of organophosphorus pesticides from aqueous solution by Zr-Based MOFs of UiO-67. *ACS Appl Mater Interfaces* **2015**, 7 (1), 223–231.
38. X. Zhu, B. Li, J. Yang, et al. Effective adsorption and enhanced removal of organophosphorus pesticides from aqueous solution by Zr-Based MOFs of UiO-67. *ACS Appl Mater Interfaces* **2015**, 7 (1), 223–231.
39. C. Sarkar, C. Bora, S.K. Dolui. Selective Dye Adsorption by pH Modulation on Amine-Functionalized Reduced Graphene Oxide–Carbon Nanotube Hybrid. *Ind Eng Chem Res* **2014**, 53 (42), 16148–16155.
40. Freundlich Equation - an overview | ScienceDirect Topics <https://www.sciencedirect.com/topics/agricultural-and-biological-sciences/freundlich-equation> (accessed Jul 5, 2021).
41. M.J. Iqbal, M.N. Ashiq. Adsorption of dyes from aqueous solutions on activated charcoal. *J Hazard Mater* **2007**, 139 (1), 57–66.
42. S. Chakravarty, A. Mohanty, T.N. Sudha, et al. Removal of Pb(II) ions from aqueous solution by adsorption using bael leaves (*Aegle marmelos*). *J Hazard Mater* **2010**, 173 (1–3), 502–509.
43. M. Chin, C. Cisneros, S.M. Araiza, et al. Rhodamine B degradation by nanosized zeolitic imidazolate framework-8 (ZIF-8). *RSC Advances*. 2018, pp 26987–26997.
44. F.C. Wu, R.L. Tseng, R.S. Juang. Initial behavior of intraparticle diffusion model used in the description of adsorption kinetics. *Chemical Engineering Journal* **2009**, 153 (1–3), 1–8.
45. W. Rudzinski, W. Plazinski. Studies of the kinetics of solute adsorption at solid/solution interfaces: On the possibility of distinguishing between the diffusional and the surface reaction kinetic models by studying the pseudo-first-order kinetics. *Journal of Physical Chemistry C* **2007**, 111 (41), 15100–15110.
46. Y. Hao, Z. Wang, J. Gou, Z. Wang. Kinetics and thermodynamics of diquat removal from water using magnetic graphene oxide nanocomposite. *Can J Chem Eng* **2015**, 93 (10), 1713–1720.
47. S. Harabi, S. Guiza, A. Álvarez-Montero, et al. Adsorption of Pesticides on Activated Carbons from Peach Stones. *Processes* **2024**, Vol. 12, Page 238 **2024**, 12 (1), 238.
48. T. Motúzová, I. Koutník, M. Vráblová. Removal of Pesticides from Water by Adsorption on Activated Carbon Prepared from Invasive Plants. *Water Air Soil Pollut* **2024**, 235 (12), 1–18.